Forensic Science International 261 (2016) 129–136

Contents lists available at ScienceDirect

Forensic Science International

journal homepage: www.elsevier.com/locate/forsciint

Impact sites representing potential bruising locations associated with rearward falls in children

Raymond Dsouza [1], Gina Bertocci *

Injury Risk Assessment and Prevention (iRAP) Laboratory, Bioengineering Department, University of Louisville, KY, USA

ARTICLE INFO

Article history:
Received 12 August 2015
Received in revised form 6 November 2015
Accepted 7 February 2016
Available online 15 February 2016

Keywords:
Biomechanics
Child abuse
Bruising
Injury assessment
Force sensor
Childhood falls

ABSTRACT

Children presenting multiple unexplained bruises can be an early sign of physical abuse. Bruising locations on the body can be an effective indicator of abusive versus accidental trauma. Additionally, childhood falls are often used as falsely reported events in child abuse, however, characterization of potential bruising locations associated with these falls does not exist. In our study we used a 12-month old pediatric anthropomorphic test device (ATD) adapted with a custom developed force sensing skin to predict potential bruising locations during rearward falls from standing. The surrogate bruising detection system measured and displayed recorded force data on a computerized body image mapping system when sensors were activated. Simulated rearward fall experiments were performed onto two different impact surfaces (padded carpet and linoleum tile over concrete) with two different initial positions (standing upright and posteriorly inclined) so that the ATD would fall rearward upon release. Findings indicated impact locations, and thus the potential for bruising in the posterior plane primarily within the occipital head and posterior torso regions.

1. Introduction

The United States has one of the worst records among developed nations in deaths related to child abuse and neglect [1]. On average between four and seven child fatalities occur daily because of child abuse and neglect in the U.S. [2]. Child abuse is a leading cause of fatality in children up to 4 years of age; an estimated 1520 children are fatally injured annually as a result of child abuse [2]. Infants (less than 1 year in age) are the most vulnerable to abuse and have the highest rate of fatalities of all age groups [2].

Bruising in children is often visually apparent and is frequently an early manifestation of a child's abusive environment. Accidental bruising is infrequently observed in infants, due to their low degree of independent mobility [3]. Bruising locations and bruising patterns (constellation of individual bruise locations throughout the body) provide a "roadmap" documenting a child's exposure to impact. Health care professionals and law enforcement officials often have to address the question of likelihood that a child's presenting injuries are compatible with history provided by the care giver. If injuries were distinguishable between accidental and abusive trauma, presenting abused children could be diverted from being reintroduced into their abusive environments which often result in further harm or death [4].

Previous studies have retrospectively highlighted differences in bruising patterns observed clinically, to provide a better understanding of skin findings in children that maybe at a high risk of abuse in their current environment [3,5–11]. However, the ability to predict potential bruising locations associated with falsely reported events (e.g. short distance falls) in child abuse does not exist and could prove useful in the distinction between abusive and accidental injuries. Rearward falls could be experienced by children who are in the early development stage of independent mobility. This type of fall (falling rearwards and impacting the head occipital region) may represent greater potential for injury because there is no protective or righting reflex in a rearward fall as in a sideways or forwards fall [12].

In our study we used a bruising detection system to identify potential bruising patterns in simulated rearward falls from standing using a child surrogate representative of a 12-month old child (stage of early independent mobility). The bruising detection system consists of a pediatric anthropomorphic test device (ATD) adapted with a custom developed force sensing skin

* Corresponding author at: Room 204 Health Sciences Research Tower, 500 S. Preston St, Louisville, KY 40202, USA. Tel.: +1 502 852 0296.
E-mail addresses: raymond.dsouza@louisville.edu (R. Dsouza), g.bertocci@louisville.edu (G. Bertocci).
[1] Room 110 Instructional Building B., 500 S. Preston St, Louisville, KY 40202, USA. Tel.: +1 502 852 0279.

http://dx.doi.org/10.1016/j.forsciint.2016.02.012
0379-0738/

that is linked to display recorded force data on a computerized body mapping image system when the force sensors are activated [13]. Simulated rearward fall experiments were performed onto two different impact surfaces with two different initial positions, while recording ATD impact sites so as to predict potential bruising locations.

The purpose of this study is to provide a "roadmap" of the child surrogate's contact exposure during specific fall events and to identify whether variations in the fall parameters (impact surface, initial position) lead to differences in impact locations. Our goal was to characterize potential bruising locations or patterns associated with a common childhood fall.

2. Methods

The surrogate bruising detection system (SBDS), consisting of the 12 month old CRABI ATD (10 kg mass) fitted with a force sensing skin and associated data acquisition hardware and analysis software, was used to predict potential bruising patterns in simulated fall scenarios. The CRABI ATD head weight is 2.6 kg (5.8 lbs), and body weight is 10 kg (22 lbs), thus the head represents ~26% of the overall body weight. The sensing skin of the SBDS consists of 132 force sensing resistive sensors (the head had a total of 32 sensors) enveloping the surface of the ATD that is divided into seven regions including the head, anterior torso, posterior torso, upper arm (arm), lower arm (forearm), upper leg (thigh), and lower leg (shank). Each body region was covered with an individualized custom sensor array/pattern. The resistive sensors in the sensing skin were connected to the data acquisition system through a voltage divider circuit. Additional details of the SBDS and its individual components are described in earlier publications [13,14].

The SBDS was used to assess potential bruising locations on the ATD body during a series of rearward fall experiments simulating falls.

2.1. Test setup

The ATD was placed in an upright standing (orthostatic) position on ground level using a suspension system supported by a tripod with a manually operated release mechanism to allow the ATD to fall under the effect of gravity. The ATD has a standing height of 74.7 cm (29.4 in.). Fall experiments were conducted using two different initial conditions. The ATD was suspended such that the ATD was positioned at an angle of 20 degrees (scenario 1 – upright initial condition) and 30° (scenario 2 – posteriorly inclined initial position) (two different initial positions) to the vertical so that the ATD would fall rearward upon release (Fig. 1, scenario 1). The ATD's CG height above ground level differed for each fall scenario (Table 1). In both fall scenarios the ATD's feet were in contact with the ground at the start of the fall. To initiate a fall, the release mechanism was activated which released the ATD allowing it to fall rearward.

Prior to each fall, ATD joint angles were adjusted using a goniometer to ensure repeated positioning in all tests. Additionally, joint stiffness was calibrated to manufacturer specifications whereby the joints were tightened until the friction was just sufficient to support the weight of the limb against gravity. Two impact surfaces were evaluated for each fall scenario: (1) padded carpet over a wood subfloor and (2) linoleum tile over a concrete subfloor. The carpet surface consisted of a 1.3 cm (1/2 in.) thick open loop carpet placed over 1.0 cm (3/8 in.) thick foam padding. The carpet and padding were placed over a 1.9 cm (3/4 in.) thick plywood platform 183 cm × 91.5 cm (6 ft × 3 ft) built to standard building codes with 5.1 cm × 10.2 cm (2 in. × 4 in.) joists, spaced 40.6 cm (16 in.) on center. 0.32 cm (1/8 in.) linoleum tile was adhered to a concrete subfloor for the second impact surface used in the fall experiments.

Fig. 1. ATD in an upright initial position (scenario 1) for simulated rearward fall experiments.

2.2. Data acquisition and analysis

The SBDS's sensors consist of force sensing resistors whose outputs were fed to the data acquisition system through a voltage divider circuit to convert resistance to voltage. Data acquisition hardware (National Instruments, Austin, TX) was used to capture and convert the analog sensor output. Multifunctional input/output data acquisition cards (PCI-6225; National Instruments) acquired, conditioned and digitized the sensor output signals. The National Instruments PCI-6225 data acquisition card is capable of measuring 80 single ended analog channels at a 16 bit resolution and a sample rate of 250 kS/s. A personal computer served as the platform for the data acquisition hardware. Graphical programming software (Labview 2010; National Instruments, Austin, TX) was used to acquire and display sensor output in a manner that relates sensor location to body region. A Virtual Instrument (VI) was developed to accomplish this objective. An active 3D (3-dimensional) body map image representing the ATD served as a graphical interface and was developed using Labview (National Instruments) software. The body image was discretely mapped to the sensors on the ATD such that active sensor outputs (those which have been impacted) and their locations were displayed on the computerized body map image. Sensor outputs in terms of force magnitude were color-coded, designating a pre-determined force range so as to aid in the quick overview of locations with high intensities of impact. A personal computer served as the platform for the data acquisition hardware. A threshold force of 4.5 N (≈1 lb or 5% of ATD body weight) was used to establish the onset of contact between the ATD and impact surface.

Table 1
Evaluated fall scenarios, ATD center of gravity (CG) position and impact surfaces.

Fall type and initial position	CG height (cm/in)	Surface type
Rearward – upright	46 (18)	Padded carpet on wood Linoleum tile on concrete
Rearward – posteriorly inclined	38 (15)	Padded carpet on wood Linoleum tile on concrete

Eight trials of each simulated rearward fall scenario (upright and posteriorly inclined initial positions) were conducted onto two different impact surfaces (padded carpet and linoleum) (Table 1). A total of 32 fall experiments were conducted.

2.3. Motion capture

All falls were captured using a digital video camera (120 frames per second) to record overall fall dynamics. The camera was positioned so that the line of sight was perpendicular to the ATD sagittal plane. This allowed for qualitative assessment of fall dynamics.

2.4. Statistical methods

The data was assessed for normality and a two-way analysis of variance (ANOVA) test was used to analyze impact forces on body regions to determine if initial position and impact surface factors led to significant differences. Additionally, post hoc tests were conducted to further examine where significant differences existed ($p \leq 0.05$). Individual sensors were grouped by body region. Body regions were defined as head, anterior torso, posterior torso, left and right upper arm, left and right lower arm, left and right upper leg, and left and right lower leg.

3. Results

3.1. Fall dynamics

All fall scenarios generated contact in one body plane (posterior) and no other body planes contacted the impact surface. The hyperextended neck while the ATD was in the initial position (Figs. 2 and 3) was a direct result of suspending the ATD from the head. After the fall was initiated (trigger of release mechanism), the head would return to a neutral position during the fall, before the ATD made contact with the floor (as can be seen in the 200 ms time lapse images in Figs. 2 and 3).

3.1.1. Rearward falls – upright initial position

In the upright falls (scenario 1), the ATD fell after release into a squatting position with hips and knees flexed (200 ms – Fig. 2), then rotated rearward (posteriorly) about the feet. The first body region impacting the floor surface was the posterior pelvis (320 ms – Fig. 2), followed by the posterior aspect of the head and torso (450 ms – Fig. 2). Subsequent to initial impact, the ATD head and torso rebound upward and rearward off the floor surface. This led to nearly simultaneous secondary impact of the posterior head and torso (500 ms – Fig. 2). The body map images (Fig. 2) correspond to the video capture images describing areas of contact during the fall sequence. Since we were primarily concerned with the initial impact event, data associated with the secondary impact following rebound was not evaluated. Additionally, there were no observable differences in fall dynamics across surface type.

3.1.2. Rearward falls – posteriorly inclined initial position

In the inclined falls (scenario 2), the ATD torso fell downward, flexing at the hip, followed by rearward rotation of the torso about the hip (hip extension). As the torso was rotating posteriorly about the hip, neck extension occurred allowing the head to rotate posteriorly. The first body regions contacting the floor surface were the posterior pelvis and upper legs (200 ms – Fig. 3). The pelvis then rebounded, while the head and torso continued to rotate rearwards (350 ms – Fig. 3). Finally the occipital region of the head and posterior torso impacted the floor surface with the head leading the torso (450 ms – Fig. 3). Similar to the upright fall scenario, there were no visual differences in fall dynamics across surface type for the inclined falls. There was reasonable agreement between the body map images and video images of the fall sequence (Fig. 3).

3.2. Contact forces

The occipital region of the head and posterior torso were the two common body regions to impact the floor surface during all conducted falls. The mean peak impact force for the head (1995 N ± 162) and posterior torso (1050 N ± 154) were the highest

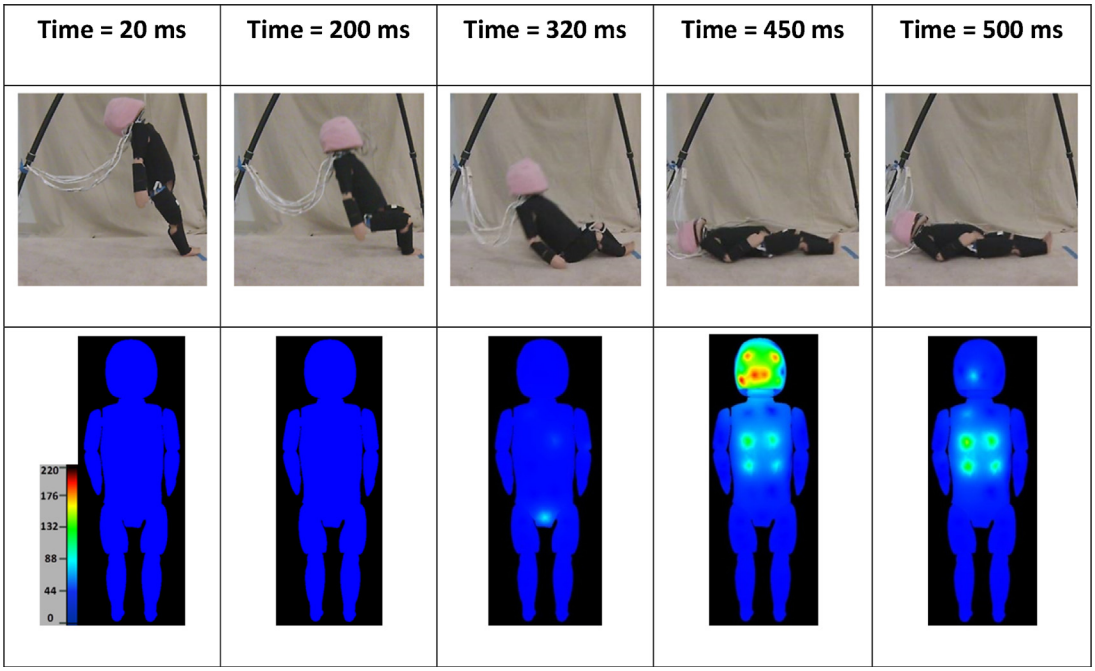

Fig. 2. Frame sequences showing video capture of the upright initial position fall onto the carpet surface and SBDS body map images at corresponding time intervals. The body map images show the posterior ATD where the colors and intensities vary depending on the level of force (N) imparted to specific regions during the fall event.

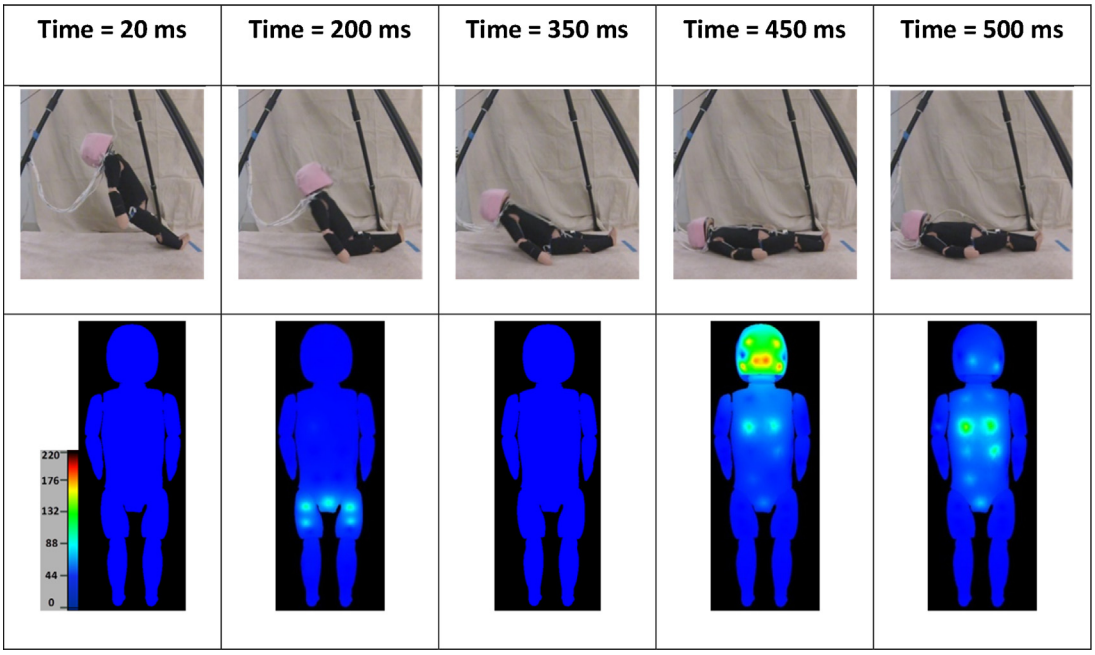

Fig. 3. Frame sequences showing video capture of the inclined initial position fall onto the carpet surface and SBDS body map images at corresponding time intervals. The body map images show the posterior ATD where the colors and intensities vary depending on the level of force (N) imparted to specific regions during the fall event.

in falls having an upright initial position onto the linoleum over concrete surface. The lowest mean peak impact force to the head (1050 N ± 79) occurred during the falls having a posteriorly inclined initial position with impact onto the carpet over wood surface. The lowest mean peak impact force to the posterior torso (244 N ± 61) occurred during falls with an upright initial position onto the carpet over wood surface (Fig. 4).

Head forces significantly differed across falls of varying initial position and impact surface type, $F(3,28) = 78.13$, $p < .001$, $\omega = 0.95$. Both main effects of position and surface for head force were statistically significant indicating that head force differs between falls onto concrete and carpet $F(1,28) = 118.49$, $p < .001$, $\omega = 0.89$ and between falls with an upright and inclined initial position $F(1,28) = 106.46$, $p < .001$, $\omega = 0.89$. The interaction effect of surface and position was also significant $F(1,28) = 9.59$, $p < .05$, $\omega = 0.51$, indicating that head force measured during impact onto different surfaces was influenced by initial position. Post hoc Tukey's HSD tests indicated that head impact forces generated in both the concrete upright fall type and carpet inclined were statistically significant from all other fall types ($p < .001$). However, the concrete inclined and carpet upright fall types did not differ significantly ($p > 0.05$).

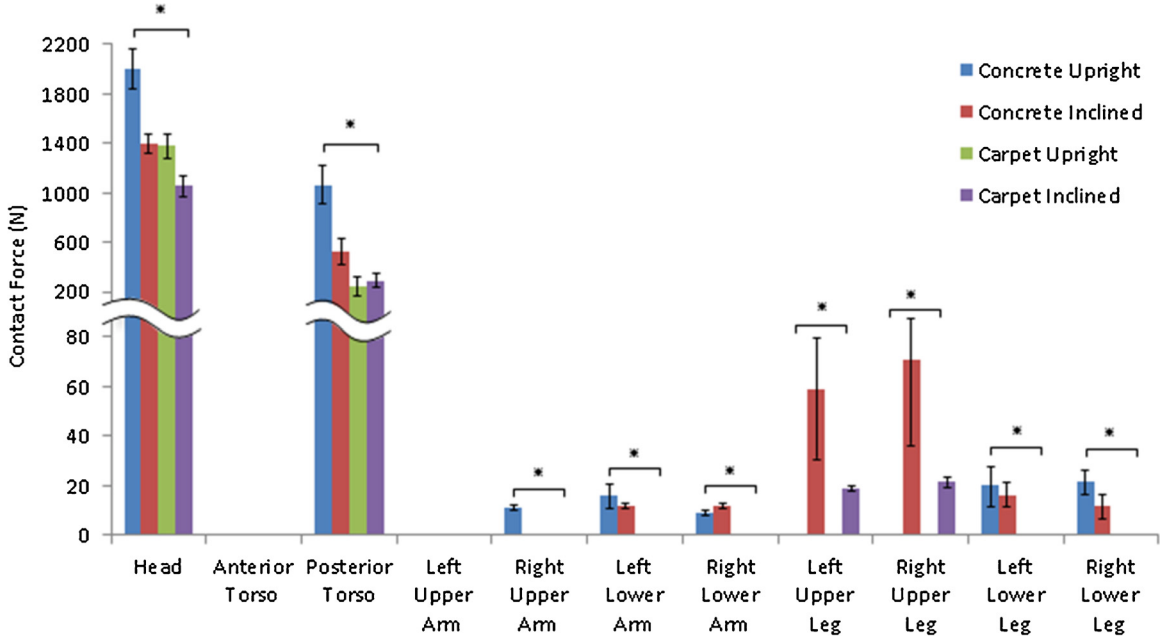

Fig. 4. Mean (8 trials) peak contact force (N) for each body region in various fall scenarios. *Statistically significant difference ($p \leq 0.05$) within the same body region.

Posterior torso forces significantly differed across falls of varying initial position and impact surface type, $F(3,28) = 79.56$, $p < .001$, $\omega = 0.95$. Both main effects of position and surface for posterior torso force were statistically significant indicating that posterior torso force differs between falls onto concrete and carpet $F(1,28) = 158.85$, $p < .001$, $\omega = 0.92$ and between falls with an upright and inclined initial position $F(1,28) = 32.82$, $p < .001$, $\omega = 0.73$. The interaction effect of surface and position was also significant $F(1,28) = 47.01$, $p < .05$, $\omega = 0.79$, indicating that posterior force measured for different impact surfaces is moderated by initial position. Post hoc Tukey's HSD tests indicated that both the concrete upright and concrete inclined fall type were statistically significant from all other fall types ($p < .001$). However, the carpet upright and carpet inclined fall types did not differ significantly ($p > 0.05$).

3.3. Potential bruising regions

3.3.1. Linoleum over concrete

The regions of maximum recorded force by the SBDS for the upright and inclined rearward falls onto linoleum on concrete surface show a difference in locations of impact (Fig. 5). The occipital region of the head and the posterior torso reflect the majority of the impact forces with the lower leg and lower arm showing minor forces. The posterior regions of the upper legs only observed contact in the inclined falls. The inclined falls appear to have no force imparted to the topmost region of the posterior torso in comparison to the upright falls.

3.3.2. Carpet over wood

The regions of maximum recorded force by the SBDS for the upright and inclined rearward falls onto carpet on wood surface show variation in locations of impact (Fig. 6). The occipital region of the head and the posterior torso again reflect the majority of the impact forces, while the posterior regions of the upper legs only observed contact in the inclined falls. The inclined falls also appear to have no force imparted to the topmost region of the posterior torso in comparison to the upright falls.

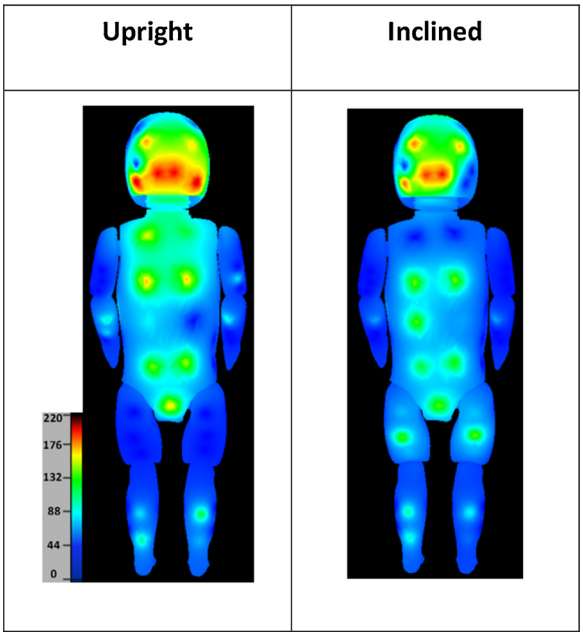

Fig. 5. Maximum impact force across 8 trials for each initial position scenario as recorded by the SBDS for rearward falls onto linoleum over concrete surface. The body map images show the posterior ATD where the colors and intensities vary dependent on the level of force (N) imparted to specific regions during the fall event.

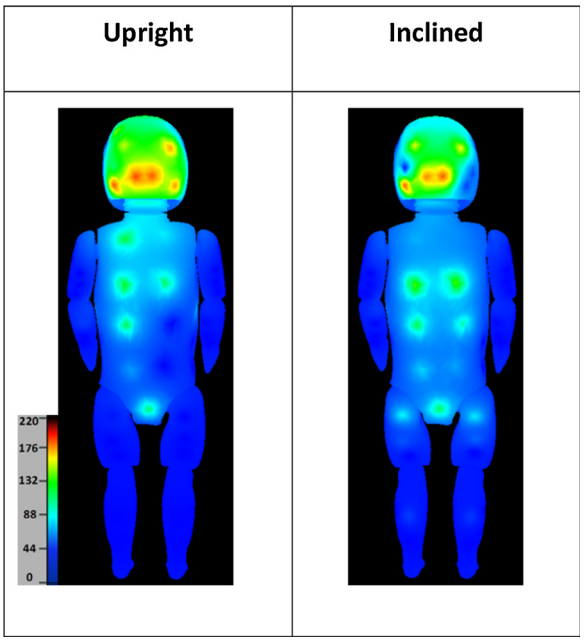

Fig. 6. Maximum impact force in across 8 trials for each initial position scenario as recorded by the SBDS for rearward falls onto carpet on wood surface. The body map images show the posterior ATD where the colors and intensities vary dependent on the level of force (N) imparted to specific regions during the fall event.

4. Discussion and conclusion

4.1. Dynamics

For the fall dynamics, we primarily analyzed the initial contact with the impact surface and any secondary or rebound impacts were disregarded. Prior studies [15–17] have shown that differences in initial position, fall dynamics and impact surfaces in fall experiments using the CRABI 12 ATD have a notable effect on recorded outcome measures. For this reason we chose to explore two initial positions and two impact surfaces in our fall experiments. There were observed differences in fall dynamics between the two initial positions (upright and inclined). In the upright falls, the ATD fell after release into a squatting position with hips and knees flexed, and then rotated rearward about the feet. These fall dynamics closely resemble the dynamics of a previous study by Thompson et al. [15] where feet-first free falls from three fall heights were simulated using the CRABI 12 onto five impact surfaces to determine the influence of fall environment characteristics on head injury risk outcomes. In 46 cm (18 in.) falls, Thompson et al. [15] found similar ATD dynamics, where the first major impact with the ground surface occurred at the pelvis followed by the torso and then head.

Fall experiments showed no observable differences in fall dynamics between the two impact surfaces. This may be as a result of the feet always being in contact with the floor surface from the start of the falls and therefore minimizing relative movement between the feet and surface in all experiments. The lack of relationship between impact surface and fall dynamics in our experiments is similar to the findings of Thompson et al. [15] which revealed no differences in fall dynamics in 46 cm (18 in.) falls onto 5 different impact surfaces (padded carpet, playground foam, linoleum over wood, linoleum over concrete, wood) having varying frictional properties.

4.2. Forces

The mean peak head impact force (1995 N ± 162) was the highest in falls having an upright initial position onto the linoleum over concrete surface and the lowest mean peak head impact force (1050 N ± 79) occurred during the falls having a posteriorly inclined initial position with impact onto the carpet over wood surface. Using the CRABI 12 ATD to assess head injury risk in experiments over three fall heights and five surfaces, Thompson et al. [15] found falls onto linoleum over concrete and carpet over wood from 46 cm (18 in.) generated peak resultant linear head accelerations of 89 *g* and 37 *g*, respectively. Based upon the ATD head accelerations and head mass of 2.6 kg (5.8 lb), calculated head impact forces for the Thompson et al. [15] study result in 2305 N (±567) and 971 N (±299) for falls onto linoleum over concrete and carpet over wood respectively.

Prange et al. [18] dropped cadaveric pediatric head specimens ranging in age of 1, 3 and 11 days and the CRABI 6 month old ATD head from heights of 15 cm and 30 cm onto a flat anvil while measuring head accelerations on different regions of the head (vertex, occiput, forehead, right parietal, left parietal). The pediatric head impacts for the occipital region resulted in an average peak acceleration of 39 *g* and 55 *g* for the 15 cm and 30 cm fall heights, respectively. The ATD head drop impacts resulted in accelerations of 39 *g* and 62 *g* for the 15 cm and 30 cm heights, respectively. The CRABI 6 month old has a head mass of 2.1 kg (4.6 lb) which results in a calculated head impact force of 817 N (184 lb) for the 15 cm (5.9 in.) fall height and 1275 N (±286 lb) for the 30 cm (11.8 in.) fall height.

Coats et al. [19] studied impact force and angular acceleration associated with low-height falls in infants. They developed an instrumented infant (1.5 month old) surrogate to measure the forces and 3D angular accelerations associated with falls from low heights (0.3–0.9 m) onto three impact surfaces – mattress, carpet pad, or concrete. The surrogate was dropped from a supine position with arms and legs extended to the sides of the body. Results of the study revealed peak head impact forces from surrogate drops onto concrete being significantly larger than those onto carpet ($p < 0.001$). The peak head impact force in the fall experiments was approximately 500 N for both 0.3 m (12 in.) drops onto carpet and concrete surfaces and approximately 650 N and 1000 N for the 0.6 m (24 in.) drops onto carpet and concrete respectively.

The head impact forces measured in our fall experiments in comparison to the studies described above are summarized in Table 2. Head forces associated with upright falls onto both impact surfaces in our experiments are in reasonable agreement with those reported by Thompson et al. [15] for falls using the same ATD and initial position. The head impact forces determined using data from the Prange et al. [18] and Coats et al. [19] studies are generally lower than our findings for a few reasons. Prange et al. [18] conducted head drop tests on an anvil using a smaller ATD (CRABI 6) in comparison to our testing using the whole ATD (CRABI 12) dropped onto carpet and concrete. Coats et al. [19] used a custom designed ATD which is younger in age (1.5 months) to ours (12 months) and has a neck design that is less stiff than the CRABI 12 ATD neck. In addition to the reduced neck stiffness, the lighter mass of the head and different initial position (supine) in Coats et al. [19] study reflect head forces that differ from our study. The head force in falls conducted by Thompson et al. [15] are close in comparison to ours however it should be noted that those forces were calculated from measured head accelerations and head mass and are therefore approximates of actual head forces.

4.3. Contact regions

Across all ($n = 32$) trials in all fall scenarios, the occipital head and posterior torso were the common regions of impact in rearward falls. Considering the dynamics of a rearward fall, impact in those regions was expected. For falls onto carpet over wood, the common regions of impact for both initial positions were the head and posterior torso. In addition to these common regions, sensors on the upper leg indicated impact for the inclined fall position. For falls onto linoleum over concrete, the common regions of impact for both initial positions were the head, posterior torso, lower arm and lower leg. In addition to these common regions, sensors on the upper leg indicated impact for the inclined position.

The commonality of impact to the upper legs in falls onto both surfaces for the inclined fall position is due to similar fall dynamics. In the inclined falls, the ATD fell into a seated position with legs fully extended, thus making contact on the upper leg region, whereas in the upright falls, the ATD rotated rearward while in a squat position onto the posterior torso thereby preventing upper leg contact to the floor.

When evaluating children with bruises in an effort to delineate between accidental and abusive trauma, the location, and pattern (constellation of individual bruises throughout the body) of bruising are especially important. Maguire et al. [20] conducted a review of current literature seeking to identify patterns of bruising that may be suggestive or diagnostic of abuse. The reviewed studies noted that bruises resulting from accidental trauma occurred predominantly on the anterior regions of the body, over bony prominences and were correlated to the child's level of independent mobility. In abused children the bruises tended to be larger and the most common sites were the face, neck, ear, head, trunk, buttocks, and arms.

Pierce et al. [8] studied the skin findings (bruises, lacerations, etc.) of children ages 0–4 years that were admitted to the pediatric intensive care unit of a tertiary care children's hospital where cause of injury was identified through the trauma registry as abuse or accident. Each patient's age, and skin findings including bruising, body region of skin finding, and number of skin findings were recorded. A total of 95 patients were analyzed in the study; 42 patients were exposed to abusive trauma and 53 patients were

Table 2
Comparison of head impact forces, ATD head properties and initial conditions from various fall studies.

	Our study CRABI 12	Thompson et al. [17] CRABI 12	Prange et al. [18] CRABI 6	Coats et al. [19] 1.5 month ATD
Head force – carpet (N)	1050–1375	972[a]	–	500–650
Head force – concrete (N)	1397–1995	2305[a]	817 and 1275[a,b]	1000
Head contact region	Occiput	Occiput	Occiput	Occiput[c]
Head mass (kg)	2.6	2.6	2.1	1.0
ATD initial position	Inclined, Upright	Upright	Head drop	Supine
Fall height (cm)	38, 46	46	15, 32	30, 60, 90

[a] Force calculated from measured acceleration and head mass.
[b] Drops onto an anvil surface.
[c] Assumed to be to the posterior aspect of the head (based on initial position) but not specified in study.

exposed to accidental trauma. Differences in body regions with bruising were identified for children with abusive versus accidental trauma. The face, cheek, scalp, head, and legs had bruising in patients with abusive and accidental trauma; these regions did not delineate between accident and abuse. However, bruising to the ear, neck, hands, right arm, chest and buttocks regions were predictive of abuse. All bruising to the genitourinary area and hip occurred only in patients with abusive trauma

Kemp et al. [21] described the characteristics of bruising and the extent to which these differ between children (aged < 6 years) where abuse was confirmed and those where it was excluded in children with suspected physical abuse. Data was collected from 506 children; abuse was confirmed in 350 and excluded in 156 children. Results indicated that abused children were significantly more likely to have bruising than those where abuse was ruled out. Abused children also had significantly more bruises, more bruising sites and clustering of bruises than the group where abuse was excluded. Bruising to the left ear, cheeks, neck, trunk, front of thighs, upper arms, buttocks and genitalia were found significantly more frequently in abused children, than when abuse was ruled out.

When assessing body regions of impact during simulated falls, it is important to compare ATD morphology/geometric shape to that of an infant's morphology. While the CRABI 12 ATD represents the anthropometrics and mass distribution of a 12-month-old 50th percentile infant, its morphology (external shape/geometry) may vary somewhat from that of a 12-month-old 50th percentile infant. For example, the ATD morphology does not replicate soft tissue of the buttocks region; instead in our study, the proximal posterior upper leg region of the ATD represents the buttocks. The ATD head morphology provides a reasonable replica of a 12-month child when viewed (Fig. 7) but does not include ears, nose, lips and orbital region as individual features. However, we did not observe contact or impact to the facial region in our simulated falls. Also, the ATD head morphology does not represent the caudal most aspects of the occipital region or the mandible. Thus, it would not be possible to measure and record impact to these regions.

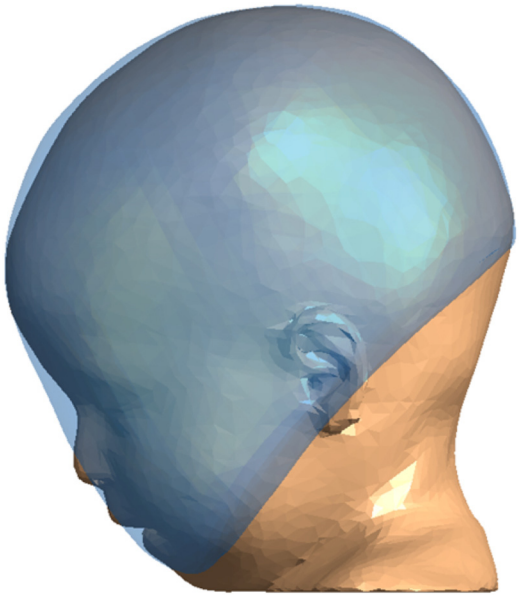

Fig. 7. Lateral comparative overlay of 11-month-old child (3D reconstruction of CT imaging) and 12-month-old CRABI ATD (transparent; blue) highlighting morphological differences in head profile. (For interpretation of the references to colour in this figure legend, the reader is referred to the web version of this article.)

The impact regions recorded in our testing in comparison to the bruising locations found on children from relevant studies described above are summarized in Table 3.

In our study we predominantly found impact to the head occipital region and posterior torso. The upper legs, lower legs and lower arms were impacted; however, magnitudes of force were lower than those measured to the occipital and posterior torso regions. Compared to previous clinical studies describing bruising locations for a range of accident types, the head and posterior torso were found to be common regions of bruising [20,21]. In contrast to Kemp et al. [21], Maguire et al. [20] and Pierce et al. [8] we did not find impact or potential for bruising to the ear region. However, Kemp et al. [21] and Maguire et al. [20] did not report fall description, mechanism or injury causation. Thus, this limits direct comparisons to those studies as our experimental findings are specific to one fall scenario. The study by Pierce et al. [8] did indicate cause of accidental trauma, however children in their study were admitted to the hospital's intensive care unit (ICU) and had severe injuries likely associated with high energy events unlike a fall from standing height. Posterior leg and posterior arm impacts were found in our experiments, but have not been recorded in clinical data because the force levels are likely below the levels to cause bruising.

5. Limitations

The biofidelity of the CRABI ATD and in particular the soft tissue biofidelity is a limitation of the SBDS. The ATD surrogate "soft tissue" consists of a heat cured vinyl plastisol that is layered with urethane foam between the outer and inner layers. The plastisol is compliant and molded to mimic the body contours representing "soft tissue". SBDS sensor measured forces are proportional to the stiffness of the underlying ATD surrogate soft tissue; therefore soft tissue biofidelity greatly influences the measured forces. However, our primary goal was to determine points of contact during various injurious events and secondarily to assess relative levels of force imparted to different regions of the body. Thus, biofidelic limitations of the surrogate soft tissue do not prevent us from meeting our goals.

Also, since the CRABI ATD was primarily designed for measuring a child's response to a high energy automotive crash environment, any findings from testing conducted with the ATD in lower deceleration events such as falls should be interpreted in light of biofidelity limitations. For example, the neck is somewhat stiffer with limited range of motion designed for frontal impacts having little or no out of plane motion. The rubber elements that attach the limbs to the ATD torso are used in the hip and shoulder joints to provide the CRABI infant-like range of motion, but are an approximation of true infant biofidelity. In addition, joints of the shoulders, elbows, hips, and knees of the ATD are limited to motion primarily in the sagittal plane. Though ATD kinematics in our simulated falls occurred primarily in the sagittal plane, any out of plane motion may lead to inaccuracies in kinematics and force measures. Varying ATD joint stiffness/properties could additionally alter fall dynamics thereby influencing impact locations and forces during falls. Additionally, we were unable to implement sensors in the neck region of the ATD given its construction (segmented rubber and aluminum disks), but based on our experimental fall dynamics, the ATD neck had a low likelihood of contact/impact during falls.

The occurrence of a bruise varies from person to person for a given application of force based on many contributing factors that affect bruise development [22–24]. Extrinsic factors such as the amount of force applied, rate of force application, and distribution of the force over larger/smaller areas are parameters that can affect the presence or absence of a bruise. Additionally, intrinsic factors

Table 3
Comparison of potential bruising locations in our study to bruising observed in previous clinical studies or reviews of clinical studies.

	Our study	Kemp et al. [21]	Maguire et al. [20]	Pierce et al. [8]
Regions of abusive bruising	–	Head, cheek, ear, neck, trunk, upper arms, front of thighs,	Head including face, front of body, ear, neck, trunk, arms, buttocks	All regions including torso, ear and neck
Regions of accidental bruising	[a]Head occipital, posterior torso, posterior upper leg, posterior lower leg, posterior lower arm	Head, Rear trunk	Head, forehead, back, abdomen, forearms, hands, buttocks, knees, shins, foot	All regions excluding torso, ear and neck

[a] Recorded impact locations that could represent potential bruising locations and are only specific to one fall type (rearward falls).

related to the physiological and anatomical structures, such as architecture of the skin, soft tissue thickness, toughness of skin, fat content, vessel fragility, and presence and depth of underlying bone add to the complexity of this physiological event [24]. Variables such as blood platelet levels, systemic blood pressure, vascular diseases and vasoactive or anticoagulant drug use in addition to nutritional and allergy related disorders can have a great influence on the presence, absence and variability in intensity of a bruise [7,24–26]. This implies that the minimum load to cause bruising, the "bruising threshold", varies across individuals. However it can be said with some degree of certainty that larger forces (applied to the same area and body location in the same individual) will be associated with a greater potential for bruising. So instead of definitively asserting the presence of a bruise, we are identifying potential bruising locations occurring within a body region under specific fall conditions.

While our findings predicted bodily impact locations, representing the potential for bruising in a rearward fall from standing using the SBDS, limitations described herein must be considered. However, the capability to predict potential bruising locations or patterns is useful when attempting to determine compatibility between a stated cause and associated skin findings in forensic analyses.

Acknowledgements

This study was funded by the National Institute of Justice (Grant No.# 2008-DD-BX-K311) and by the Office of Juvenile Justice and Delinquency Prevention (Grant No.# 2009-DD-BX-0086), Office of Justice Programs, US Department of Justice. Points of view or opinions expressed herein are those of the authors and do not necessarily represent the official position or policies of the US Department of Justice.

We would like to acknowledge Dr. Angela Thompson for her assistance in our statistical assessment of the data and help in converting CT image files to a 3D solid model. Additionally, post-mortem CT data was provided courtesy of the University of New Mexico Radiology-Pathology Center for Forensic Imaging, supported by National Institute of Justice Grant 2010-DN-BX-K205.

References

[1] G. Lenzer, J. Grochowalski, Social Justice for Children: To End Child Abuse and Violence Against Children: a National Consultation, 20th Anniversary of the Founding of the Field of Children's Studies, Children's Studies Center for Research, Policy and Public Service, Brooklyn College, City University of New York, 2012.
[2] DHHS, Child maltreatment 2013, U.S. Department of Health and Human Services, Administration for Children and Families, Washington, DC, 2013.
[3] K.W. Feldman, The bruised premobile infant: should you evaluate further? Pediatr. Emerg. Care 25 (2009) 37–39.
[4] H.W. Petska, L.K. Sheets, B.L. Knox, Facial bruising as a precursor to abusive head trauma, Clin. Pediatr. (Phila.) 52 (2013) 86–88.
[5] S. Maguire, M.K. Mann, J. Sibert, A. Kemp, Are there patterns of bruising in childhood which are diagnostic or suggestive of abuse? A systematic review, Arch. Dis. Child. 90 (2005) 182–186.
[6] N.F. Sugar, J.A. Taylor, K.W. Feldman, Bruises in infants and toddlers: those who don't cruise rarely bruise, Arch. Pediatr. Adolesc. Med. 153 (1999) 399–403.
[7] K. Kaczor, M. Clyde Pierce, K. Makoroff, T.S. Corey, Bruising and physical child abuse, Clin. Pediatr. Emerg. Med. 7 (2006) 153–160.
[8] M.C. Pierce, K. Kaczor, S. Aldridge, J. O'Flynn, D.J. Lorenz, Bruising characteristics discriminating physical child abuse from accidental trauma, Pediatrics 125 (2010) 67–74.
[9] C. Kemp, Child abuse or accident? AAP News 15 (1999), 2-d-3.
[10] J. Wedgwood, Childhood bruising, Practitioner 234 (1990) 598–601.
[11] L.K. Sheets, M.E. Leach, I.J. Koszewski, A.M. Lessmeier, M. Nugent, P. Simpson, Sentinel injuries in infants evaluated for child physical abuse, Pediatrics 131 (2013) 701–707.
[12] B. Wilkins, Head injury—abuse or accident? Arch. Dis. Child. 76 (1997) 393–397.
[13] R. Dsouza, G. Bertocci, Design and development of a force sensing skin adapted to a child surrogate to identify potential bruising locations, Technology 2 (2014) 49–54.
[14] Bertocci G. Soft tissue impact assessment device and system. U.S. Patent 8,292,830 B2: Oct 23, 2012.
[15] A.K. Thompson, G. Bertocci, M.C. Pierce, Assessment of head injury risk associated with feet-first free falls in 12-month-old children using an anthropomorphic test device, J. Trauma: Injury Infect. Crit. Care 66 (2009) 1019.
[16] A.K. Thompson, G.E. Bertocci, Paediatric bed fall computer simulation model development and validation, Comput. Methods Biomech. Biomed. Eng. 16 (2013) 592–601.
[17] A. Thompson, G. Bertocci, M.C. Pierce, Assessment of injury potential in pediatric bed fall experiments using an anthropomorphic test device, Accid. Anal. Prev. 50 (2013) 16–24.
[18] M.T. Prange, J.F. Luck, A. Dibb, C.A. Van Ee, R.W. Nightingale, B.S. Myers, Mechanical properties and anthropometry of the human infant head, Stapp Car Crash J. 48 (2004) 279–299.
[19] B. Coats, S.S. Margulies, Potential for head injuries in infants from low-height falls, J. Neurosurg. Pediatr. 2 (2008) 321–330.
[20] S. Maguire, M. Mann, Systematic reviews of bruising in relation to child abuse-what have we learnt: an overview of review updates, Evid. Based Child Health 8 (2013) 255–263.
[21] A.M. Kemp, S.A. Maguire, D. Nuttall, P. Collins, F. Dunstan, Bruising in children who are assessed for suspected physical abuse, Arch. Dis. Child. 99 (2014) 108–113.
[22] E.F. Wilson, Estimation of the age of cutaneous contusions in child abuse, Pediatrics 60 (1977) 750–752.
[23] S. Maguire, M.K. Mann, J. Sibert, A. Kemp, Can you age bruises accurately in children? A systematic review, Arch. Dis. Child. 90 (2005) 187–189.
[24] T.L. Harris, E.G. Flaherty, Bruises and skin lesions, in: C. Jenny (Ed.), Child Abuse and Neglect: Diagnosis, Treatment and Evidence, Elsevier Saunders, Canada, 2011, pp. 237–251.
[25] K. Khair, R. Liesner, Bruising and bleeding in infants and children – a practical approach, Br. J. Haematol. 133 (2006) 221.
[26] N.E.I. Langlois, G.A. Gresham, The ageing of bruises: a review and study of the colour changes with time, Forensic Sci. Int. 50 (1991) 227–238.